C. R. Palevol 9 (2010) 341–348

Contents lists available at ScienceDirect

Comptes Rendus Palevol

www.sciencedirect.com

General palaeontology

Tissue proportions and enamel thickness distribution in the early Middle Pleistocene human deciduous molars from Tighenif, Algeria

Proportions des tissus et distribution de l'épaisseur de l'émail des molaires déciduales humaines du début du Pléistocène moyen de Tighenif, Algérie

Clément Zanolli [a,*], Priscilla Bayle [a,b], Roberto Macchiarelli [a,c]

[a] *Département de préhistoire, UMR 7194, MNHN, bâtiment 140, 43, rue Buffon, 75005 Paris, France*
[b] *Research Department of Cell and Developmental Biology, University College London, Gower Street, London WC1E 6BT, UK*
[c] *Département géosciences, université de Poitiers, 40, avenue du Recteur-Pineau, 86022 Poitiers cedex, France*

ARTICLE INFO

Article history:
Received 22 February 2010
Accepted after revision 30 July 2010

Written on invitation of the Editorial Board

Keywords:
Human deciduous molars
Tissue proportions
Enamel thickness
Tighenif
Early Middle Pleistocene
Microtomography

ABSTRACT

The present study of three human upper deciduous molars from the early Middle Pleistocene site of Tighenif, Algeria, constitutes the first microtomographic-based endostructural exploration of African fossil teeth likely representative of the *Homo heidelbergensis* morph. Comparative morphological observations and 2-3D measurements describing subtle tooth organization (crown tissue proportions) and enamel thickness topography (site-specific distribution and global patterning) indicate that their virtual extracted structural signature better fits the modern human, rather than the Neanderthal condition. Accordingly, we predict that the inner structural morphology of the deciduous molars from the Middle Pleistocene western European series better fits the primitive, and not the derived Neanderthal figures.

Mots clés :
Molaires déciduales humaines
Proportions des tissus
Épaisseur de l'émail
Tighenif
Début du Pléistocène moyen
Microtomographie

RÉSUMÉ

Cette étude de trois molaires déciduales supérieures humaines du site du début du Pléistocène moyen de Tighenif, Algérie, constitue la première exploration endostructurale, basée sur un registre microtomographique, de dents africaines fossiles représentant vraisemblablement le morphe *Homo heidelbergensis*. Les observations morphologiques comparatives et les mesures 2-3D décrivant l'organisation fine de la dent (proportions des tissus de la couronne) et la topographie de l'épaisseur de l'émail (distribution sito-spécifique et patron global) indiquent que leur signature structurale virtuellement extraite est plus proche de la condition humaine moderne que de la condition néanderthalienne. Par conséquent, nous prédisons que la morphologie de la structure interne des molaires déciduales des fossiles du Pléistocène moyen d'Europe occidentale correspond mieux à la forme primitive, et non à celle dérivée, présentée par les Néandertaliens.

* Corresponding author.
E-mail address: clement.zanolli@mnhn.fr (C. Zanolli).

1631-0683/$ – see front matter
doi:10.1016/j.crpv.2010.07.019

1. Introduction

The early Middle Pleistocene human remains from Tighenif (formerly Ternifine), Algeria, were discovered between 1954 and 1956 by C. Arambourg in a sand quarry in the province of Mascara (Arambourg, 1954, 1955, 1957; Arambourg and Hoffstetter, 1954). Based on comparative biochronology, the site is currently dated to ca. 700 kyr (Geraads et al., 1986). The fossil collection, stored at the Department of Palaeontology, MNHN Paris, consists of two nearly complete mandibles (Tighenif 1 and 3), one hemimandible (Tighenif 2), a parietal fragment (Tighenif 4), and nine isolated teeth, three deciduous and six permanent, all characterized by large crown dimensions (Arambourg and Hoffstetter, 1963; Tillier, 1980).

Originally attributed to *Atlanthropus mauritanicus* (Arambourg, 1954, 1955), the remains from Tighenif have been traditionally integrated within the *Homo erectus* hypodigm (Howell, 1960; Le Gros Clark, 1964; Rightmire, 1990; Tillier, 1980; for a review, see Antón, 2003; Antón et al., 2007; Schwartz and Tattersall, 2003). Based on external dental crown features, their possible affinity to the morph represented by the Early Pleistocene specimens from Gran Dolina, Spain (Bermúdez de Castro et al., 1997), has been also noted (Schwartz and Tattersall, 2005). More recently, a revision of the fossil material assigned to *H. heidelbergensis* (Mounier et al., 2009) suggests that the amount of morphological and dimensional similarities of the sample from Tighenif justifies its allocation to this latter Afro-European taxon. Additionally, the authors (Mounier et al., 2009) point out that, because of some derived features (notably, the development of a chin-like protuberance on Tighenif 2; Schwartz and Tattersall, 2000), the Algerian material is morphologically closer to *H. sapiens* than to Neanderthals.

Because of recent methodological advances in the 3D "virtual" exploration of tooth structural morphology (in Macchiarelli et al., 2008; Smith and Tafforeau, 2008) and the current debate on the evolutionary significance of the taxon-related patterns of human dental tissue organization and proportions (e.g., Bayle et al., 2010; Olejniczak et al., 2008; Smith et al., 2009), subtle inner morpho-structural evidence from the Algerian sample, whose taxonomic attribution and phylogenetic status remain a matter of discussion, may shed light on the still unreported condition characterizing the Early-Middle Pleistocene African dental record.

In this perspective, here we present the first results of the high-resolution noninvasive investigation of the three deciduous elements, all molars, from Tighenif (Fig. 1).

2. Material and methods

The specimens, originally described by Tillier (1980) for their external size and morphology, represent the crown of a left and a right upper first molar (ULm1 and URm1), and of a left upper second molar (ULm2). It is likely that, in all three cases, the roots were in advanced resorption. In 2009, the specimens have been imaged by high-resolution microtomography (μCT) at the Centre de Microtomographie of the Université de Poitiers (equipment X8050-16 Viscom AG; camera 1004 × 1004), according to the following parameters: 120 kV, 0.45 mA current, 32 integrations/projection, and a projection each 0.24°. The final volumes have been reconstructed using DigiCT v.2.3.3 (DIGISENS) with an isotropic voxel size of 21.57 μm^3.

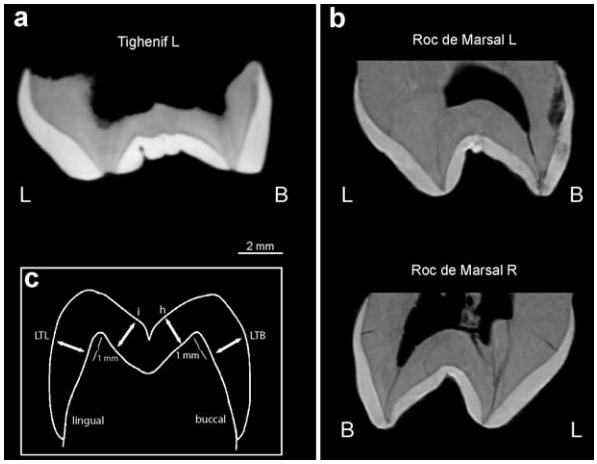

Fig. 1. Linguo-buccal virtual sections across the deciduous ULm2 from Tighenif (a) and the Um2s of the Neanderthal child of Roc de Marsal (b), and schematic representation of a molar crown indicating the enamel sites measured in this study (c, from Grine, 2005). L, lingual; B, buccal.
Fig. 1. Coupes bucco-linguales virtuelles dans la ULm2 déciduale de Tighenif (a) et les Um2s de l'enfant Néanderthalien de Roc de Marsal (b), et représentation schématique d'une couronne de molaire montrant la localisation des mesures d'émail de cette étude (c, Grine, 2005). L, lingual ; B, buccal.

Using Avizo 6.1 (Visualization Sciences Group Inc.) and MPSAK 2.9 (in Dean and Wood, 2003), a semi-automatic threshold-based segmentation has been carried out following the half-maximum height (HMH; Spoor et al., 1993) and the region of interest thresholding methods (ROI-Tb protocol; Fajardo et al., 2002). From that step, the fossil crowns have been virtually uncapped (Olejniczak et al., 2008) and each tissue visualized separately. In order to assess tissue proportions, the blank volume between the cervical reference plane and the dentine was then considered as dentine. Despite their degree of mineralization and the local extent of occlusal dental wear (notably, on the ULm1), in all cases the endostructural signal was quite distinct, with high contrasts between enamel and dentine (Fig. 1a).

The following seven linear, surface, and volumetric variables describing tooth tissue proportions were digitally measured or calculated: Ve, the volume of the enamel cap (mm^3); Vcdp, the volume of the coronal dentine, including the coronal aspect of the pulp chamber (mm^3); Vc, the total crown volume, including enamel, dentine, and pulp (mm^3); SEDJ, the enamel-dentine junction (EDJ) surface (mm^2); Vcdp/Vc (= (Vcdp/Vc) × 100), the percent of coronal volume that is dentine and pulp (%); 3D AET (=Ve/SEDJ), the three-dimensional average enamel thickness (mm); 3D RET (=3D AET/$(Vcdp)^{1/3}$), the scale-free three-dimensional relative enamel thickness (for methodological details, see Kono, 2004; Martin, 1985; Olejniczak et al., 2008).

The results from the virtual analysis of the three specimens from Tighenif have been directly compared to the microtomographic-based quantitative evidence from the poorly worn maxillary deciduous molars of the

Neanderthal child of Roc de Marsal (Bayle et al., 2009a) and to a modern human dental sample (MH) from a medieval cemetery at Usseau, France, including 4 virtually unworn upper m1s and 3 upper m2s. All comparative specimens have been scanned with the same equipment as the Tighenif sample (for methodological considerations, see Olejniczak et al., 2007).

Limitedly to the m2s of Tighenif and Roc de Marsal, four additional measures of radial enamel thickness have been taken on the buccol-lingual (BL) virtual sections through the mesial cusps-dentine horns and compared to the estimates obtained on histological ground by Grine, 2005 (Fig. 1). On the Algerian m2, dentine is exposed on the tip of the cusps, but lateral wall enamel is intact. Accordingly, apical enamel thickness has not been measured, while specific estimates have concerned the buccal and the lingual sides, respectively. The variables are as follows: LTB, the maximum linear enamel thickness assessed on the buccal side of the mesio-buccal cusp, perpendicular to the EDJ at a point approximately 1 mm cervical to the dentine horn apex; LTL, the maximum linear enamel thickness assessed on the lingual side of the mesio-lingual cusp, perpendicular to the EDJ at a point approximately 1 mm cervical to the dentine horn apex; *h*, the maximum linear thickness of occlusal enamel assessed on the mesio-buccal cusp, perpendicular to the EDJ; *i*, the maximum linear thickness of occlusal enamel assessed on the mesio-lingual cusp, perpendicular to the EDJ (for methodological details, see Grine 2005; Kono, 2004; Martin, 1985).

For all 2D and 3D measures, intra- and inter-observer tests for accuracy run by two observers provided differences of $\leq 4\%$.

3. Results

The ULm1 from Tighenif is extensively worn (stage 4; Smith, 1984), with evident occlusal dentine patches. The URm1, which still preserves a small root fragment, is slightly less worn (stage 3; Smith, 1984), with at least three flattened cusps and spread dentine spots. Compared to the m1s, the ULm2 is only poorly worn (stage 1-2; Smith, 1984), with small dentine exposure on lingual cusps (Fig. 2). This latter crown bears three accessory traits: one small cuspule-like structure inserted between paracone and metacone, originally described as a double buccal groove (Tillier, 1980: 415); a small cuspule set on the mesial aspect of the paracone; and a Carabelli's trait on the mesio-lingual aspect (grade 5 of the ASUDA scoring system; Turner et al., 1991).

The virtual reconstruction of the outer enamel surface (OES) and of the EDJ of the three specimens is shown in Fig. 3. The EDJ is an interface playing a crucial role during tooth development, as most of the morphological features expressed at the OES are mapped on the EDJ at the embryonic stage, while others are the results of overgrowth only affecting the enamel surface (Skinner et al., 2008). Moreover, the virtual exploration of the EDJ morphology allows the identification of subtle features of potential taxonomic value (Macchiarelli et al., 2006; Skinner et al., 2008).

Despite some size differences between the smaller left and the larger right m1s (B-L: 9.9 vs. 10.7 mm, respectively; Tillier, 1980), and the extensive occlusal dental wear partially masking the lingual half of the left crown, a comparative analysis of their EDJ surfaces reveals a close morphological resemblance in terms of subtle structural features. This is true for the general appearance of the basin ridges and, limitedly to paracone and metacone, for the cusp pattern and the relatively high and protrusive marginal ridges. The intact EDJ of the second molar clearly shows the imprint on the dentine of the three accessory traits appearing at the OES (Fig. 3). Notably, at the

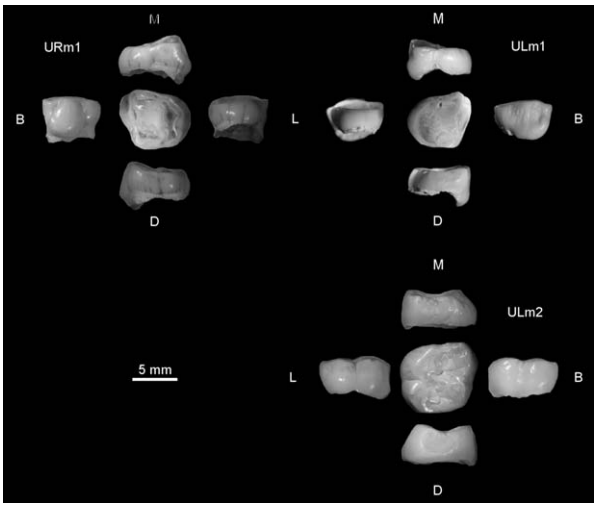

Fig. 2. The three deciduous upper molars from Tighenif (coll. MNHN, Paris). M, mesial; D, distal; B, buccal; L, lingual. For each tooth, the central image is the occlusal view.
Fig. 2. Les trois molaires déciduales supérieures de Tighenif (coll. MNHN, Paris). M, mésial ; D, distal ; B, buccal ; L, lingual. Pour chaque dent, l'image centrale est en vue occlusale.

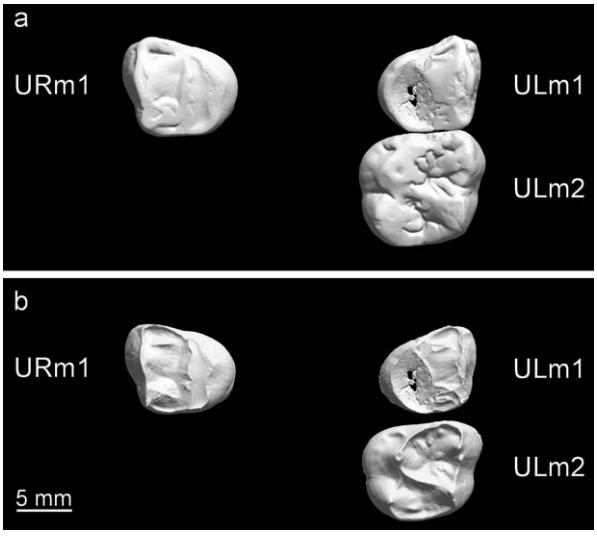

Fig. 3. Virtual reconstruction of the outer enamel (a) and the enamel-dentine junction (b) surfaces of the three deciduous molars from Tighenif in occlusal view.
Fig. 3. Reconstructions virtuelles de la surface externe de l'émail (a) et de la surface de la jonction émail-dentine (b) des trois molaires déciduales de Tighenif en vue occlusale.

EDJ, the external feature between paracone and metacone corresponds to a small but distinct cuspule. Conversely, the single mesial cuspule hardly appreciable occlusally because of wear, corresponds to two lesser cuspule-like traits lying on the mesial marginal ridge (Fig. 4).

Comparative dental tissue proportions in Tighenif, the Neanderthal child from Roc de Marsal, and a modern human sample (MH) are shown in Table 1. Limitedly to the m1s from Tighenif, notably the left one, it should be pointed out that the values concerning the volume of the enamel cap (Ve), the volume of the coronal dentine (Vcdp), the total crown volume (Vc), the Vcdp/Vc percent ratio, and, of course, the enamel thickness estimates (3D AET and RET), are affected by occlusal dental wear and have to be considered as minimum estimates only.

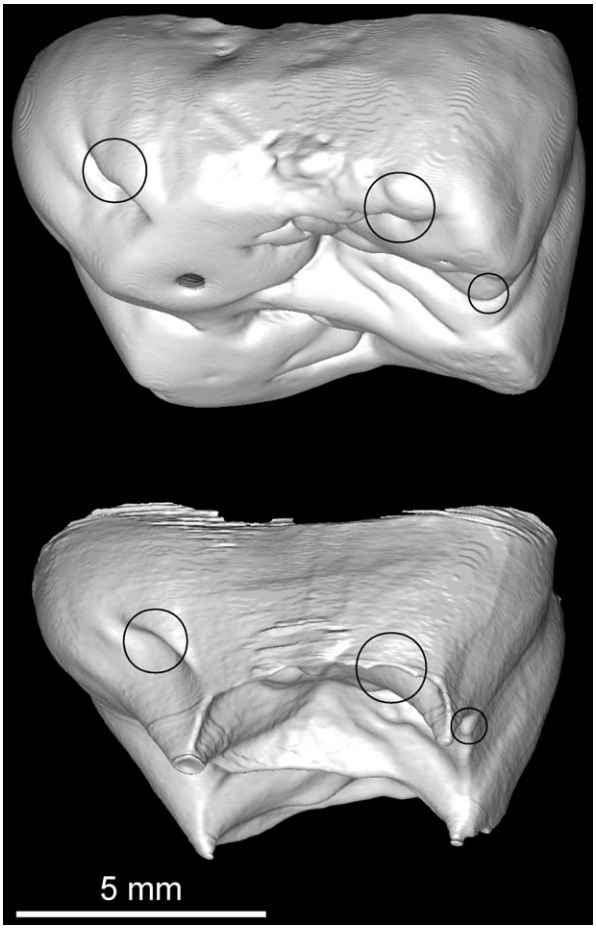

Fig. 4. Occluso-mesial view of the virtually reconstructed outer enamel (top) and the enamel-dentine junction (bottom) of the ULm2 from Tighenif showing three accessory cuspules, two at the level of the paracone (separately circled on the mesio-buccal aspect, to the right) and a Carabelli's trait (circled on the mesio-lingual aspect, to the left). See the text (Results) for description.

Fig. 4. Vue occluso-mésiale des reconstructions virtuelles de la surface externe de l'émail (haut) et de la jonction émail-dentine (bas) de la ULm2 de Tighenif montrant trois cuspules accessoires, deux au niveau du paracone (encerclées séparément sur la face mésio-buccale, à droite) et un tubercule de Carabelli (encerclé sur la face mésio-linguale, à gauche). Voir le texte (Résultats) pour la description.

Despite the absolute and relative amount of enamel loss respectively testified by their low enamel cap volumes (Ve) and high Vcdp/Vc ratios, both m1s from Tighenif display a significantly larger total crown volume (Vc) compared to the Neanderthal and the modern specimens, as well as a larger volume of coronal dentine, including the coronal aspect of the pulp chamber (Vcdp). For Vcdp, Neanderthals are typically characterized by a coronal dentine significantly larger than observed in extant humans (Bayle, 2008; Bayle et al., 2009a; Macchiarelli et al., 2006; Olejniczak et al., 2008). In Tighenif m1s, a difference of 17.2% and 15.2% should be noted between the crowns for Vc and Vcdp, respectively, the right crown being the larger one, as already noticed for the bucco-lingual and mesio-distal diameters by Tillier (1980). In these two crowns, the same pattern is also shown by the portion of the EDJ surface (SEDJ) which is unaffected by wear. With this respect, the Algerian fossil specimens show the absolutely largest values within the comparative sample considered in this study, associated to a lesser difference of 7.6% between the left (smaller) and the right surfaces.

In terms of inner structural morphology, a clearer pattern for the Tighenif dental sample emerges from the analysis of the Um2 (Table 1). In this case, all volumes of the African specimen systematically and significantly exceed the comparative estimates, as does the EDJ surface. However, in relative proportions, the percent of coronal volume that is dentine and pulp (Vcdp/Vc: 62%) closely fits the modern figure (range: 59–62%), not the estimate for the immature from Roc de Marsal (66%).

As noted above, both 3D AET and RET values for the Um1s from Tighenif are biased, while those assessed for the second molar are reliable. For the 3D average enamel thickness (AET), the value of the Algerian specimen falls again within the modern variation range represented in our study, in any case well above the figures of Roc de Marsal. Conversely, Tighenif occupies an intermediate position for the 3D relative enamel thickness (RET).

For all linear variables describing cuspal enamel thickness through the protocone-paracone virtual section (LTB, LTL, h, i), the values of the maxillary m2 from Tighenif are systematically closer to the modern human figures (data from Grine, 2005) than to the estimates obtained for both Roc de Marsal's m2s (Table 2). In all cases, fossil and modern, the enamel is thicker on the lingual aspect of the protocone than on the buccal side of the paracone (LTL > LTB). However, while in Tighenif and the reference modern sample the same topographic pattern is distinctly shown also by the maximum linear thickness of occlusal enamel (i > h), in the available Neanderthal representative the difference between protocone and paracone is slight, with no directional pattern.

For each fossil (Tighenif and Roc de Marsal) and modern (three specimens) m2 crown, a 3D virtual perspective in five views of the enamel thickness topographic variation is rendered in Fig. 5 by means of a thickness-related colour scale (in mm). This visualization technique maps the local enamel thickness on the outer enamel surface and permits to comparatively appreciate the structural contrasts (Kono, 2004; Macchiarelli et al., 2008, 2009).

Table 1
Linear, surface, and volumetric variables virtually assessed on three deciduous upper molars from Tighenif (ULm1, URm1, and ULm2), the Neanderthal child from Roc de Marsal (from Bayle et al., 2009a), and some modern human molar crowns (MH).
Tableau 1
Variables linéaires, surfaciques, et volumétriques estimées virtuellement pour les trois molaires déciduales supérieures de Tighenif (ULm1, URm1 et ULm2), l'enfant néandertalien de Roc de Marsal (Bayle et al., 2009a), et plusieurs couronnes de molaires humaines modernes (MH).

	Ve (mm^3)	Vcdp (mm^3)	Vc (mm^3)	SEDJ (mm^2)	Vcdp/Vc (%)	3D AET (mm)	3D RET
Um1							
Tighenif L	42.79*	178.25*	221.04*	152.41*	81*	0.28*	4.99*
R	56.77*	210.16	266.94*	164.88*	79*	0.34*	5.79*
Roc de Marsal L	50.60	126.76	177.37	120.25	71	0.42	8.38
R	51.80	127.79	179.59	116.89	71	0.44	8.80
Modern humans							
MH-1	60.63	101.90	162.53	101.86	63	0.60	12.74
MH-2	74.20	107.87	182.07	110.71	59	0.67	14.08
MH-3	53.89	90.03	143.93	101.41	63	0.53	11.86
MH-4	53.37	100.90	154.27	98.02	65	0.54	11.70
Um2							
Tighenif L	158.95	259.13	418.08	212.91	62	0.75	11.71
Roc de Marsal L	108.43	214.11	322.54	182.14	66	0.60	9.95
R	111.08	214.68	325.76	183.94	66	0.60	10.09
Modern humans							
MH-5	104.43	168.94	273.37	147.76	62	0.71	12.78
MH-6	134.89	191.69	326.58	152.96	59	0.88	15.29
MH-7	117.25	175.60	292.85	153.50	60	0.76	13.64

See the text (Materials and methods) for description of the variables. L, left; R, right. *, affected by occlusal wear.

Comparative cartographies clearly evidence the whole similarity between the Algerian fossil and the modern human pattern in enamel topographic distribution, while the absolutely and relatively thin-enameled Neanderthal specimen clearly sets apart. Nonetheless, while in the three modern m2s measured in the present study (range total crown volume: 273–327 mm^3) the thickest enamel is found mesially, at the base of the protocone (1.25 mm), in

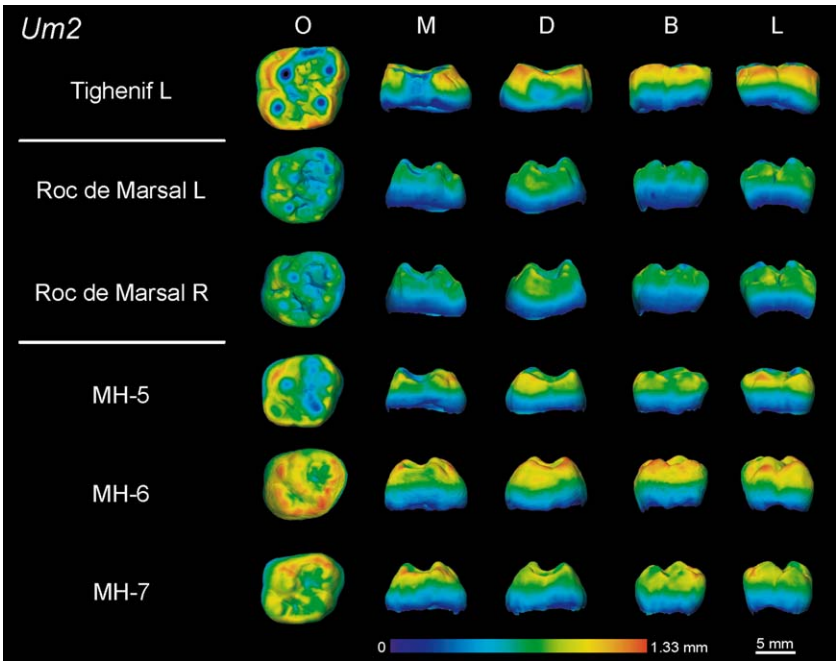

Fig. 5. Microtomographic-based comparative maps of enamel thickness variation of the deciduous Um2s from Tighenif, the Neanderthal child of Roc de Marsal, and three modern humans (MH). All teeth are shown as left and are given in occlusal (O), mesial (M), distal (D), buccal (B), and lingual (L) views. The enamel topographic variation is rendered by a thickness-related pseudo-colour scale (ranging from "thin" dark-blue to "thick" red). Isolated dark spots correspond to occlusal wear. L, left; R, right.
Fig. 5. Cartographies comparatives virtuelles des variations d'épaisseur de l'émail des molaires déciduales de Tighenif, de l'enfant néandertalien de Roc de Marsal, et de trois spécimens modernes (MH). Toutes les dents sont présentées comme des dents gauches et sont montrées en vues occlusale (O), mésiale (M), distale (D), buccale (B) et linguale (L). La variation topographique d'épaisseur de l'émail est représentée par une échelle en fausses couleurs (allant du bleu foncé « fin » au rouge « épais »). Les zones noires isolées correspondent à l'usure occlusale. L, gauche ; R, droite.

Table 2
Linear variables (all in mm) measured on the 2D sections passing through protocone and paracone and dentine horns for Tighenif and Roc de Marsal Um2s. The modern human estimates (MH; mean values ± 1 s.d.) are from Grine (2005).
Tableau 2
Variables linéaires (toutes en mm) mesurées sur les sections 2D passant par le protocone, le paracone et les cornes de dentine des Um2s de Tighenif et Roc de Marsal. Les estimations pour les spécimens modernes (MH, valeurs moyennes ± 1σ) proviennent de Grine (2005).

	Tighenif L	Roc de Marsal L	Roc de Marsal R	MH ($N = 10$)
LTB	1.08	0.74	0.69	1.11 ± 0.16
LTL	1.23	0.80	0.81	1.36 ± 0.26
h	0.80	0.68	0.57	0.86 ± 0.19
h	0.91	0.59	0.60	0.98 ± 0.19

See the text (Materials and methods) and Fig. 1c for description of the variables. L, left; R, right.

Tighenif (418 mm^3) it corresponds to the distal marginal ridge (1.28 mm).

4. Discussion and conclusions

Following the original description and interpretation of the isolated dental sample from Tighenif, because of their proportions, external morphology, occlusal and interproximal wear patterns, it is likely that the three deciduous upper molars are from the same individual (Tillier, 1980). With this respect, the qualitative and quantitative results derived from the present microtomographic-based 3D virtual analysis of their endostructure do not reject such interpretation. In particular, while the left and right first molars show some linear, surface, and volumetric differences (Tillier, 1980 and present Table 1), their enamel-dentine junction surfaces fit in terms of morphological details. Nonetheless, the preservation conditions of the two specimens do not allow a conclusive statement on this matter, and additional finer structural analyses, likely via phase contrast synchrotron radiation microtomography (see Smith and Tafforeau, 2008), should test this point in the future.

Our attempt to characterize the pattern of tooth tissue proportions and enamel thickness distribution of the morph represented by this early Middle Pleistocene North African sample faced the unavoidable limits represented by the preservation conditions of the m1s and, of course, small sample size. Nonetheless, it is noteworthy that, besides the evidence from a few Neanderthals (Bayle, 2008; Bayle et al., 2009a, 2010; Bondioli et al., 2010; Macchiarelli et al., 2006, 2007; Toussaint et al., 2010) and even fewer anatomically modern fossil specimens (Bayle et al., 2009b, 2010), the extent of deciduous tooth endostructural variation is simply unreported for any Early and Middle Pleistocene human extinct taxon. At the best of our knowledge, the only 3D estimates of tissue proportions available so far concern two *H. erectus s.s.* permanent molars from Trinil, whose relative enamel volumes better fit the modern human rather than the Neanderthal condition (Smith et al., 2009).

Currently available 3D imaging evidence shows that, compared to the extant human condition reported so far, Neanderthal deciduous teeth possess relative thinner enamel, absolutely and relatively larger dentine volumes, larger and more complex enamel-dentine junction, larger pulp chambers, thicker roots (Bayle, 2008; Bayle et al., 2009a, 2010; Bondioli et al., 2010; Macchiarelli et al., 2006, 2007; Toussaint et al., 2010). In this perspective, certainly for the upper m2, our results allow a preliminary assessment of the primitive inner structural condition characterizing the deciduous molars of the early Middle Pleistocene North African groups likely related to *H. heidelbergensis*.

The comparative analysis of the percent of the crown volume that is dentine and pulp (Vcdp/Vc) shows that, relative to the enamel, the proportion of dentine and pulp is higher in the Neanderthal specimen considered in the present study, but more balanced in both Tighenif and the modern reference sample. Limitedly to the structural organization of the lower deciduous molars, but not of the incisors (Bayle et al., 2010), the same pattern distinguishes Neanderthals from both anatomically modern fossil and extant humans (Bayle, 2008; Bayle et al., 2009a, 2009b, 2010; Macchiarelli et al., 2006, 2007; Toussaint et al., 2010). Accordingly, Tighenif is closer to the latter groups.

A growing body of evidence also shows that, while the Neanderthal and modern human dentitions are comparable in terms of total volume of enamel (e.g., Olejniczak et al., 2008), Neanderthals possess a more complex EDJ surface (Macchiarelli et al., 2006; Toussaint et al., 2010; for the permanent molars, see Skinner et al., 2008) and greater dentine proportions (Bayle, 2008; Bayle et al., 2009a), finally resulting in lower average (AET) and relative (RET) enamel thickness values (on historical ground, cf. Smith and Zilberman, 1994). Here again, the evidence from Tighenif fits the modern human condition. In fact, the differences in enamel thickness topography recorded on the Tighenif's m2 between the thicker protocone and the thinner paracone are in accordance with the functional pattern expected for the modern deciduous upper molars, likely related to the development of a helicoidal occlusal wear plane (Grine, 2005).

In sum up, present comparative morphological observations and 2-3D measures concerning the topographic repartition pattern and global distribution of the enamel (site-specific thickness and total volume), and the tooth organization as reflected by crown tissue proportions (notably, those between dentine-pulp and enamel), all indicate that, in relative terms, the structural signature virtually extracted from the ca. 700 kyr deciduous teeth from Tighenif closely resembles the modern human condition. While, at this preliminary stage, these results do not legitimate any conclusive statement on the taxonomic status of the Algerian sample because of the current lack of similar information on other Early-Middle Pleistocene samples (except for the developmental study of the dentition of the *sapiens*-like Middle Pleistocene child from Jebel Irhoud, Morocco; Smith et al., 2007), they, nonetheless, identify the likely primitive deciduous tooth pattern for both Neanderthals and anatomically modern humans.

Accordingly, based also on recent suggestions about the role of genetic drift in shaping Neanderthal morphology (e.g., Weaver, 2009), we predict that the inner struc-

tural morphology of the deciduous molars from Middle Pleistocene western European series, such as Tautavel, in France, or Atapuerca Sima de los Huesos (SH), in Spain, better fits the primitive, not the derived Neanderthal condition.

Acknowledgements

We are indebted to G. Clément and D. Geffard-Kuriyama for their kind invitation to contribute to this special volume and for their successful organizational effort. We thank C. Argot and H. Lelièvre for having granted access to the fossil specimens from Tighenif discussed in this paper, as well as for the technical support provided in order to make easier their preliminary record at the MNHN, Paris. D. Grimaud-Hervé contributed to the original planning of this ongoing project. The microtomographic record of the teeth from Tighenif has been realized at the Centre de Microtomographie (CdM) of the Univ. of Poitiers thanks to the collaboration and under the supervision of A. Mazurier (Etudes Recherches Matériaux, Poitiers). Comparative data used in this study come from microtomographic analyses of modern and fossil human teeth realized at the ESRF beamline ID 17, Grenoble (Roc de Marsal, courtesy of J.-J. Cleyet-Merle [Musée National de Préhistoire, Les Eyzies-de-Tayac]) and the CdM, Poitiers (modern reference teeth, courtesy of M. Bessou, B. Maureille, P. Murail [Univ. Bordeaux 1], J.-L. Kahn [Institut d'Anatomie of Strasbourg], and J. Braga [Univ. Toulouse III]). For technical and scientific collaboration, we acknowledge A. Bravin, A. Mazurier, C. Nemoz, P. Sardini, P. Tafforeau. Research supported by the MNHN (to C.Z.), the CNRS, the Nespos Society (https://nespos-live01.pxpgroup.com/display/openspace/Home), the Univ. of Poitiers (to R.M.), the EVAN project (EU FP6 Marie Curie Actions MRTN-CT-2005-019564) and the Fyssen Foundation (to P.B.).

References

Antón, S.C., 2003. Natural history of *Homo erectus*. Yearb. Phys. Anthop. 46, 126–170.

Antón, S.C., Spoor, F., Fellmann, C.D., Swisher III, C.C., 2007. Defining *Homo erectus*: size considered. In: Henke, W., Tattersall, I. (Eds.), Handbook of paleoanthropology. Springer, New York, pp. 1655–1695.

Arambourg, C., 1954. L'hominien fossile de Ternifine (Algérie). C. R. Acad. Sci. Paris 239, 893–895.

Arambourg, C., 1955. A recent discovery in human paleontology: *Atlanthropus* of Ternifine (Algeria). Am. J. Phys. Anthropol. 13, 191–201.

Arambourg, C., 1957. Récentes découvertes de paléontologie humaine réalisées en Afrique du Nord française (L'*Atlanthropus* de Ternifine - L'Hominien de Casablanca). In: Clark, J.D., Cole, S. (Eds.), Proceedings of the third Panafrican congress on prehistory. Chatto and Windus, London, pp. 186–194.

Arambourg, C., Hoffstetter, R., 1954. Découverte en Afrique du Nord de restes humains du Paléolithique inférieur. C. R. Acad. Sci. Paris 239, 72–74.

Arambourg, C., Hoffstetter, R., 1963. Le gisement de Ternifine. Arch. Inst. Pal. Hum. 32, 1–190.

Bayle, P., 2008. Proportions des tissus des dents déciduales chez deux individus de Dordogne (France) : l'enfant Néanderthalien du Roc de Marsal et le spécimen du Paléolithique supérieur final de La Madeleine. Bull. Mem. Soc. Anthrop. Paris 20, 151–163.

Bayle, P., Braga, J., Mazurier, A., Macchiarelli, R., 2009a. Dental developmental pattern of the Neanderthal child from Roc de Marsal: a high-resolution 3D analysis. J. Hum. Evol. 56, 66–75.

Bayle, P., Braga, J., Mazurier, A., Macchiarelli, R., 2009b. High-resolution assessment of the dental developmental pattern and characterization of tooth tissue proportions in the late Upper Paleolithic child from La Madeleine France. Am. J. Phys. Anthropol. 138, 493–498.

Bayle, P., Macchiarelli, R., Trinkaus, E., Duarte, C., Mazurier, A., Zilhão, J., 2010. Dental maturational pattern and dental tissue proportions in the early Upper Paleolithic child from Abrigo do Lagar Velho Portugal. Proc. Natl. Acad. Sci. USA 107, 1338–1342.

Bermúdez de Castro, J.M., Arsuaga, J.L., Carbonell, E., Rosas, A., Martínez, I., Mosquera, M., 1997. A hominid from the Lower Pleistocene of Atapuerca, Spain: possible ancestor to Neandertals and modern humans. Science 276, 1392–1395.

Bondioli, L., Bayle, P., Dean, M.C., Mazurier, A., Puymerail, L., Ruff, C., Stock,.J.T., Volpato, V., Zanolli, C., Macchiarelli, R., 2010. Morphometric maps of long bone shafts and dental roots for imaging topographic thickness variation. Am. J. Phys. Anthropol. 142, 328–334.

Dean, M.C., Wood, B., 2003. A digital radiographic atlas of great apes skull and dentition. In: Bondioli, L., Macchiarelli, R. (Eds.), Digital archives of human paleobiology. ADS Solutions, Milan (CD-ROM).

Fajardo, R.J., Ryan, T.M., Kappelman, J., 2002. Assessing the accuracy of high-resolution X-ray computed tomography of primate trabecular bone by comparisons with histological sections. Am. J. Phys. Anthropol. 118, 1–10.

Geraads, D., Hublin, J.J., Jaeger, J.J., 1986. The Pleistocene hominid site of Ternifine Algeria: new results on the environment, age, and human industries. Quat. Res. 25, 380–386.

Grine, F.E., 2005. Enamel thickness of deciduous and permanent molars in modern *Homo sapiens*. Am. J. Phys. Anthropol. 126, 14–31.

Howell, F.C., 1960. European and Northwest African Middle Pleistocene hominids. Curr. Anthrop. 1, 195–232.

Kono, R., 2004. Molar enamel thickness and distribution patterns in extant great apes and humans: new insights based on a 3-dimensional whole crown perspective. Anthrop. Sci. 112, 121–146.

Le Gros Clark, W.E., 1964. The fossil evidence for human evolution: an introduction to the study of palaeoanthropology, 2nd ed. University of Chicago Press, Chicago, 201 p.

Macchiarelli, R., Bondioli, L., Debénath, A., Mazurier, A., Tournepiche, J.F., Birch, W., Dean, M.C., 2006. How Neanderthal molar teeth grew. Nature 444, 748–751.

Macchiarelli, R., Mazurier, A., Volpato, V., 2007. L'apport des nouvelles technologies à l'étude des Néandertaliens. In: Vandermeersch, B., Maureille, B. (Eds.), Les Néandertaliens. Biologie et cultures. Comité des Travaux Historiques et Scientifiques, Paris, pp. 169–179.

Macchiarelli, R., Bondioli, L., Mazurier, A., 2008. Virtual dentitions: touching the hidden evidence. In: Irish, J.D., Nelson, G.C. (Eds.), Technique and application in dental anthropology. Cambridge University Press, Cambridge, pp. 426–448.

Macchiarelli, R., Mazurier, A., Illerhaus, B., Zanolli, C., 2009. *Ouranopithecus macedoniensis* (Mammalia, Primates Hominoidea): virtual reconstruction and 3D analysis of a juvenile mandibular dentition (RPl-82 and RPl-83). Geodiversitas 31, 851–864.

Martin, R., 1985. Significance of enamel thickness in hominoid evolution. Nature 314, 260–263.

Mounier, A., Marchal, F., Condemi, S., 2009. Is *Homo heidelbergensis* a distinct species? New insight on the Mauer mandible. J. Hum. Evol. 56, 219–246.

Olejniczak, A.J., Tafforeau, P., Smith, T.M., Temming, H., Hublin, J.J., 2007. Technical note: compatibility of microtomographic imaging systems for dental measurements. Am. J. Phys. Anthropol. 134, 130–134.

Olejniczak, A.J., Smith, T.M., Feeney, R.N., Macchiarelli, M., Mazurier, R., Bondioli, A., Rosas, L., Fortea, A., de la Rasilla, J., Garcia-Tabernero, M., Radovcic, A., Skinner, J., Toussaint, M., Hublin, J.J., 2008. Dental tissue proportions and enamel thickness in Neandertal and modern human molars. J. Hum. Evol. 55, 12–23.

Rightmire, G.P., 1990. The evolution of *Homo erectus*. Cambridge University Press, New York, 260 p.

Schwartz, J.H., Tattersall, I., 2000. The human chin revisited: what is it and who has it? J Hum. Evol. 38, 367–409.

Schwartz, J.H., Tattersall, I., 2003. The human fossil record. In: Craniodental morphology of genus *Homo* (Africa and Asia), vol. 2. Wiley-Liss, Hoboken, 616 p.

Schwartz, J.H., Tattersall, I., 2005. The human fossil record. In: Craniodental morphology of early hominids (genera *Australopithecus*, *Paranthropus*, *Orrorin*), and overview, vol. 4. Wiley-Liss, Hoboken, 561 p.

Skinner, M.M., Wood, B.A., Boesch, C., Olejniczak, A.J., Rosas, A., Smith, T.M., Hublin, J.J., 2008. Dental trait expression at the enamel-dentine junction of lower molars in extant and fossil hominoids. J. Hum. Evol. 54, 173–186.

Smith, H.B., 1984. Patterns of molar wear in hunter-gatherers and agriculturalists. Am. J. Phys. Anthropol. 63, 39–56.
Smith, T.M., Tafforeau, P., 2008. New visions of dental tissue research: tooth development, chemistry, and structure. Evol. Anthrop. 17, 213–226.
Smith, P., Zilberman, U., 1994. Thin enamel and other tooth components in Neanderthals and other hominids. Am. J. Phys. Anthropol. 95, 85–87.
Smith, T.M., Tafforeau, P., Reid, D.J., Grün, R., Eggins, S., Boutakiout, M., Hublin, J.J., 2007. Earliest evidence of modern human life history in North African early *Homo sapiens*. Proc. Natl. Acad. Sci. USA 104, 6128–6133.
Smith, T.M., Olejniczak, A.J., Kupczik, K., Lazzari, V., de Vos, J., Kullmer, O., Schrenk, F., Hublin, J.-J., Jacob, T., Tafforeau, P., 2009. Taxonomic assessment of the Trinil molars using non-destructive 3D structural and development analysis. PaleoAnthrop. 2009, 117–129.
Spoor, C.F., Zonneveld, F.W., Macho, G.A., 1993. Linear measurements of cortical bone and dental enamel by computed tomography: applications and problems. Am. J. Phys. Anthropol. 91, 469–484.
Tillier, A.M., 1980. Les dents d'enfant de Ternifine (Pléistocène moyen d'Algérie). L'Anthropologie 84, 413–421.
Toussaint, M., Olejniczak, A.J., El Zaatari, S., Cattelain, P., Flas, D., Letourneux, C., Pirson, S., 2010. The Neandertal lower right deciduous second molar from Trou de l'Abîme at Couvin. Belgium. J. Hum. Evol. 58, 56–67.
Turner II, C.G., Nichol, C.R., Scott, G.R., 1991. Scoring procedures for key morphological traits of the permanent dentition: the Arizona State University dental anthropology system. In: Kelly, M.A., Larsen, C.S. (Eds.), Advances in dental anthropology. Wiley-Liss, New York, pp. 13–31.
Weaver, T.D., 2009. The meaning of Neandertal skeletal morphology. Proc. Natl. Acad. Sci. U. S. A. 106, 16028–16033.